ISSN 1063-7761, Journal of Experimental and Theoretical Physics, 2015, Vol. 121, No. 1, pp. 27–34. © Pleiades Publishing, Inc., 2015.
Original Russian Text © V.M. Aul'chenko, M.N. Achasov, A.Yu. Barnyakov, K.I. Beloborodov, A.V. Berdyugin, A.G. Bogdanchikov, A.A. Botov, A.V. Vasil'ev, V.B. Golubev, T.V. Dimova, V.P. Druzhinin, L.V. Kardapol'tsev, A.S. Kasaev, A.N. Kirpotin, D.P. Kovrizhin, I.A. Koop, A.A. Korol', S.V. Koshuba, A.S. Kupich, A.P. Lysenko, K.A. Martin, A.E. Obrazovskii, E.V. Pakhtusova, E.A. Perevedentsev, A.L. Romanov, Yu.A. Rogovskii, S.I. Serednyakov, Z.K. Silagadze, A.N. Skrinskii, I.K. Surin, Yu.A. Tikhonov, A.G. Kharlamov, D.A. Shtol', 2015, published in Zhurnal Eksperimental'noi i Teoreticheskoi Fiziki, 2015, Vol. 148, No. 1, pp. 34–41.

NUCLEI, PARTICLES, FIELDS, GRAVITATION, AND ASTROPHYSICS

Study of the $e^+e^- \to \pi^+\pi^-\pi^0$ Process in the Energy Range 1.05–2.00 GeV

V. M. Aul'chenko[a,b], M. N. Achasov[a,b], A. Yu. Barnyakov[a,b], K. I. Beloborodov[a,b], A. V. Berdyugin[a,b], A. G. Bogdanchikov[a], A. A. Botov, A. V. Vasil'ev[a,b], V. B. Golubev[a,b], T. V. Dimova[a,b]*, V. P. Druzhinin[a,b], L. V. Kardapol'tsev, A. S. Kasaev[a], A. N. Kirpotin[a], D. P. Kovrizhin[a,b], I. A. Koop[a–c], A. A. Korol'[a,b], S. V. Koshuba[a,b], A. S. Kupich[a,b], A. P. Lysenko[a], K. A. Martin[a,b], A. E. Obrazovskii[a], E. V. Pakhtusova[a], E. A. Perevedentsev[a,b], A. L. Romanov[a,b], Yu. A. Rogovskii[a,b], S. I. Serednyakov[a,b], Z. K. Silagadze[a,b], A. N. Skrinskii[a], I. K. Surin[a], Yu. A. Tikhonov[a,b], A. G. Kharlamov[a,b], and D. A. Shtol'[a]

[a] *Budker Institute of Nuclear Physics, Siberian Branch, Russian Academy of Sciences, pr. Akademika Lavrent'eva 11, Novosibirsk, 630090 Russia*

* *e-mail: baiert@inp.nsk.su*

[b] *Novosibirsk State University, ul. Pirogova 2, Novosibirsk, 630090 Russia*

[c] *Novosibirsk State Technical University, Novosibirsk, 630092 Russia*

Received October 20, 2014

Abstract—The cross section for the $e^+e^- \to \pi^+\pi^-\pi^0$ process in the energy range 1.05–2.00 GeV has been measured using the data collected in the experiment with the Spherical Neutral Detector (SND) at the VEPP-2000 e^+e^- collider. The obtained results on the cross section are in good agreement with previous measurements by the SND at the VEPP-2M collider and BABAR, but have a better accuracy.

DOI: 10.1134/S1063776115060023

1. INTRODUCTION

The cross section for the $e^+e^- \to \pi^+\pi^-\pi^0$ process at the c.m. energies $\sqrt{s}$ below 1.05 GeV is described by the sum of the contributions from $\omega(782)$ and $\phi(1020)$ vector resonances. The cross section and parameters of these resonances were measured in many experiments with a high accuracy of 1–2%. The cross section above the $\phi(1020)$ resonance is determined primarily by the contributions from $\omega(1420)$ (ω') and $\omega(1650)$ (ω'') excited vector states. The parameters of these resonances were measured with a large error and should be determined more accurately. The $e^+e^- \to \pi^+\pi^-\pi^0$ process at energies above 1.05 GeV was studied for the first time in the experiment with the DM2 detector [1]. Later, more accurate measurements were performed in the experiment with the Spherical Neutral Detector at the VEPP-2M e^+e^- collider for $\sqrt{s} < 1.4$ GeV [2] and in the BABAR experiment for $\sqrt{s} < 3$ GeV [3]. It should be noted that the DM2 and BABAR measurements contradict each other. The main aim of this work was to measure the cross section for the $e^+e^- \to \pi^+\pi^-\pi^0$ process in the energy range from 1.05 to 2.00 GeV.

2. DETECTOR AND EXPERIMENT

The Spherical Neutral Detector (SND) is a universal nonmagnetic detector installed at the VEPP-2000 e^+e^- collider [4]. The main systems of the detector were described in detail in [5]. The vacuum chamber of the collider is surrounded by a track system, which consists of a nine-layer drift chamber and a one-layer proportional chamber both placed in a common gas volume. The solid angle of the track system is 94% of 4π and the resolutions in the azimuth and polar angles are 0.45° and 0.8°, respectively. There is the system of nine threshold Cherenkov counters for identification of kaons. The most important part of the detector is a three-layer spherical electromagnetic calorimeter consisting of 1630 NaI(Tl) crystals. The solid angle of the calorimeter is 90% of 4π, the energy resolution for photons is $\sigma_E/E = 4.2\%/\sqrt[4]{E[\text{GeV}]}$, and the angular resolution is about 1.5°. A muon system consisting of proportional tubes and plane scintillation counters is placed outside the calorimeter.

The experiments with the SND detector at the VEPP-2000 collider began in 2010. In this work, we use the data obtained in 2011 when scanning the energy range from 1.05 to 2.00 GeV with a step of 20–25 MeV (40 points). The total luminosity collected in this experiment is about 22 pb^{-1}.

3. LUMINOSITY MEASUREMENT

To measure the luminosity in this analysis, we used e^+e^- elastic scattering

$$e^+e^- \longrightarrow e^+e^-. \quad (1)$$

We selected events with two or more charged particles where two particles with the highest energies leave the beam interaction region of the collider (the distance from the axis of the beams to the nearest point on the track is $R_{1,2} < 0.5$ cm, the z coordinate of this point is $|z_{1,2}| < 10$ cm, and $|z_1 - z_2| < 1.5$ cm) and have the polar angle θ in the range from 40° to 140°. The azimuth and polar angles of these particles should satisfy the conditions of collinearity: $|180° - |\phi_1 - \phi_2|| < 7°$ and $|180° - (\theta_1 + \theta_2)| < 15°$, and their energies should be in the range of $(0.75–1.3)E_b$, where E_b is the energy of the beam.

The visible cross section σ_{ee} for the $e^+e^- \longrightarrow e^+e^-$ process under the above selection conditions was calculated by the Monte Carlo simulation. The parameters of the primary particles and the total cross section for the $e^+e^- \longrightarrow e^+e^-$ process were calculated with the BHWIDE event generator [6], and the response of the detector was simulated with a code based on the GEANT4 toolkit [7]. The simulation took into account changes in the state of the detector and in the background conditions during the collection of events.

The total luminosity L at each energy point was determined by the formula $L = N_{ee}/\sigma_{ee}$, where N_{ee} is the number of the selected experimental events of the $e^+e^- \longrightarrow e^+e^-$ process. The statistical error of the measurement of the luminosity at each energy point was no more than 0.3%. The systematic error of the measurement of the luminosity is determined by the statistics of simulated events (1%) and uncertainty caused by the selection condition (1.7%). The theoretical uncertainty of the BHWIDE generator is no more than 0.2% [8]. As a result, the total error of the measurement of the luminosity is 2%.

4. EVENT SELECTION

To measure the cross section of the process

$$e^+e^- \longrightarrow \pi^+\pi^-\pi^0 \quad (2)$$

we selected the events satisfying the following criteria: an event has two charged particles originating the beam interaction region (the distance from the axis of the beams to the nearest point on the track is $R_{1,2} < 0.5$ cm, the z coordinate of this point is $|z_{1,2}| < 10$ cm and $|z_1 - z_2| < 1.5$ cm) and two photons with energies above 30 MeV. To suppress the beam background and the background from electrodynamic processes ($e^+e^- \longrightarrow e^-e^+\gamma$, $e^+e^-\gamma\gamma$), we used the condition $0.3 < E_{tot}/\sqrt{s} < 0.8$ for the total energy deposition E_{tot} in the calorimeter. The selected events were subjected to the kinematic reconstruction procedure under the hypothesis that the events are attributed to the $e^+e^- \longrightarrow \pi^+\pi^-\gamma\gamma$ process; therefore, the four final particles satisfy the law of energy and momentum conservation. As a result of the kinematic reconstruction, the momenta of charged particles were determined and the energies and angles of emitted photons were refined. The quality of the kinematic reconstruction was characterized by two parameters: χ^2_R for reconstructing the common vertex and χ^2_E for satisfying the law of energy and momentum conservation. The following conditions were imposed on the refined parameters of the particles: $|z_{vtx}| < 10$ cm, where z_{vtx} is the z coordinate of the vertex of an event, polar angles of charged particles lie in the range from 30° to 150°, deviation from the collinearity of charged particles in the azimuth angle is larger than 10°, the total energy of charged particles is lower than $0.6\sqrt{s}$, and the energy deposition in the calorimeter beyond the reconstructed particles is lower than 70 MeV. In addition, we used the constraints $\chi^2_R < 40$ and $\chi^2_E < 30$ for the parameters of kinematic reconstruction.

In order to separate the events of the $e^+e^- \longrightarrow \pi^+\pi^-\pi^0$ process from the background, we analyzed the invariant-mass distribution of a pair of photons ($m_{\gamma\gamma}$). Figure 1 shows such a distribution for experimental events from the energy range of 1.3–1.4 GeV. The main background in the energy range under study comes from the $e^+e^- \longrightarrow \pi^+\pi^-\pi^0\pi^0$ and $e^+e^- \longrightarrow \pi^+\pi^-\gamma$ processes. The events of the first background process satisfy the selection conditions in the case of loss of two of four photons from decays of π^0 mesons. After the kinematic reconstruction, the two-photon mass spectrum for such events does not have a narrow peak at the mass of the π^0 meson. The spectrum is a distribution with a broad peak to the right of the π^0 peak (see the shaded histogram in Fig. 1). In the second process, dominates the contribution from radiative return to the region of the ρ-meson resonance, when a photon is emitted from the initial state and the invariant mass of a $\pi^+\pi^-$ pair is close to the mass of the ρ meson. The second photon necessary for the satisfaction of the above selection conditions appears as a result of either nuclear interaction of a pion in the calorimeter or overlapping of the beam background with an event. The $m_{\gamma\gamma}$ spectrum for events of this process that was obtained in the simulation is almost linear in the range of 80–200 MeV. The other background processes making a smaller contribution such as $e^+e^- \longrightarrow e^+e^-\gamma$, $e^+e^- \longrightarrow \mu^+\mu^-\gamma$, and $e^+e^- \longrightarrow K^+K^-\pi^0$ also have an almost linear distribution.

The experimental $m_{\gamma\gamma}$ spectrum at each energy point was approximated by the sum of the distributions of the effect and background. The distribution for the effect was taken from the simulation. The background was described by the sum of the simulated distribution for the $e^+e^- \longrightarrow \pi^+\pi^-\pi^0\pi^0$ process and a linear function. The parameters of the approximation were the

number of events of the effect $N_{3\pi}$, the number of events of the background process $N_{4\pi}$, and the parameters of the linear function. An example of the approximation is shown in Fig. 1, where it is seen that the shape of the background is poorly described to the right of the π^0 peak. Much better agreement can be obtained if two extreme channels of the distribution are removed from the approximation. However, the contraction of the approximation region for points with small statistics results in an increase of the statistical error in the determination of the background. For this reason, in order to extract the background, we used a wide interval and the difference between the numbers of events of the effect for the wide and narrow intervals, which is 2% on average, was considered as the systematic error in $N_{3\pi}$.

The number of background events $N_{4\pi}$ obtained from the approximation is in agreement with the calculation involving the experimental data on the cross section for the $e^+e^- \longrightarrow \pi^+\pi^-\pi^0\pi^0$ process. The numbers of the events of the $e^+e^- \longrightarrow \pi^+\pi^-\pi^0$ process for all energy points are presented in Table 1.

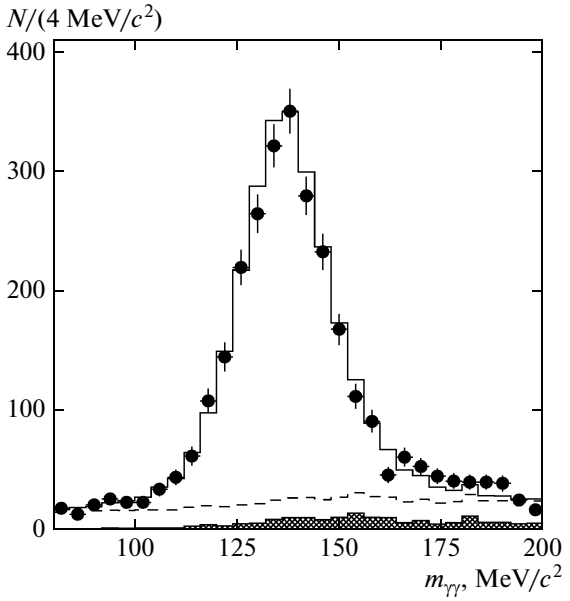

Fig. 1. Invariant mass distribution of two photons $m_{\gamma\gamma}$ for the selected experimental events (points with error bars) plotted with the use of the data at five energy points in the range of 1.3–1.4 GeV. The solid histogram is the approximation of the experimental distribution by the sum of the simulated distributions for the effect and the background from the $e^+e^- \longrightarrow \pi^+\pi^-\pi^0\pi^0$ process and a linear function. The shaded histogram is the contribution from the $e^+e^- \longrightarrow \pi^+\pi^-\pi^0\pi^0$ process. The dashed histogram is the total background.

5. DETECTION EFFICIENCY AND RADIATIVE CORRECTIONS

The detection efficiency for the process under study was determined from the simulation. The simulation involved radiative corrections to the Born cross section [9]; in particular, the emission of an additional photon from the initial state was simulated. The efficiency was determined as a function of two variables: the c.m. energy and energy of the photon emitted from the initial state (E_γ):

$$\epsilon(\sqrt{s}, E_\gamma) = \epsilon_0(\sqrt{s})\epsilon_\gamma(\sqrt{s}, E_\gamma), \qquad (3)$$

where $\epsilon_0(\sqrt{s})$ is the detection efficiency at $E_\gamma = 0$ and the function $\epsilon_\gamma(\sqrt{s}, E_\gamma)$ is normalized so that $\epsilon_\gamma(E, 0) = 1$. Figure 2a shows ϵ_0 values for all 40 energy points. Figure 2b shows the dependence $\epsilon_\gamma(E_\gamma)$ for the energy $\sqrt{s}/2 = 700$ MeV approximated by a smooth line. A nonmonotonic behavior of ϵ_0 is explained by changes in the state of the detector and background conditions during the collection of the data, which were taken into account in the simulation. In particular, a change in the number of inactive channels in the calorimeter was taken into account. The energy range under study was scanned twice: first, from low to high energies and, then, from high to low energies. The lower series of the points in Fig. 2a corresponds to down scanning.

About 10–15% of the experimental events of the process under study contain false tracks and/or photons appearing from the beam background. In order to take into account this effect in simulation, events containing background counts of the detector elements were recorded in the experiment with a special random trigger. These background counts were imposed on the events of the studied process in the simulation. Unfortunately, in the experiment in 2011, such background events were recorded irregularly. We estimated the corresponding systematic error in the efficiency of the detection as 2%.

The visible cross section $\sigma_{\text{vis},\,i} = N_{3\pi,\,i}/L_i$, where $N_{3\pi,\,i}$ is the number of events of the process under study selected at the ith energy point and L_i is the total luminosity measured at this point. The visible cross section is related to the Born cross section for the process under study σ by the integral relation

$$\sigma_{\text{vis}}(s) = \int_0^{x_{\max}} \epsilon(\sqrt{s}, xE_b)F(s, x)\sigma(s(1-x))dx, \qquad (4)$$

where $x = E_\gamma/E_b$ and $F(s, x)$ is the function describing the probability of the emission of a photon with the energy E_γ [9]. Integration is performed up to the kinematic limit

$$x_{\max} = 1 - (m_{\pi^0} + 2m_{\pi^+})^2/s.$$

Formula (4) can be represented in the traditional form

$$\sigma_{\text{vis}}(s) = \epsilon_0(s)\sigma(s)(1 + \delta(s)), \qquad (5)$$

where $\delta(s)$ is the radiative correction.

Table 1. Energy $\sqrt{s}$, total luminosity L, number of selected events $N_{3\pi}$, detection efficiency ε_0, radiative correction $1 + \delta$, and Born cross section σ at 40 scanning points obtained in 2011. The range of the radiative correction is given for five points with $\sqrt{s} \le 1.15$ GeV; the model uncertainty for the remaining points is no more than 1%

$\sqrt{s}$, GeV	L, nb^{-1}	$N_{3\pi}$	ε_0, %	$1 + \delta$	σ, nb
1.05	385.1	506.0 ± 32.5	17.5	6.73–9.82	0.98 ± 0.48 ± 0.34
1.075	548.1	618.2 ± 28.4	19.1	1.90–2.37	3.07 ± 0.27 ± 0.67
1.1	552.9	534.9 ± 31.3	18.1	1.34–1.51	3.96 ± 0.31 ± 0.58
1.125	530.5	491.9 ± 24.9	18.8	1.09–1.15	4.52 ± 0.25 ± 0.28
1.15	477.0	440.5 ± 24.4	18.0	1.00–1.03	5.13 ± 0.28 ± 0.26
1.175	532.4	520.4 ± 26.2	19.2	0.9625	5.29 ± 0.27 ± 0.23
1.2	559.9	478.0 ± 25.7	18.1	0.9330	5.07 ± 0.27 ± 0.22
1.225	562.8	574.7 ± 27.0	19.3	0.9257	5.72 ± 0.27 ± 0.25
1.25	467.0	490.7 ± 22.5	19.2	0.9229	5.93 ± 0.27 ± 0.25
1.275	501.2	489.3 ± 25.4	19.3	0.9209	5.50 ± 0.29 ± 0.24
1.3	486.2	428.7 ± 23.0	19.6	0.9233	4.87 ± 0.26 ± 0.21
1.325	553.8	486.8 ± 22.1	19.5	0.9270	4.86 ± 0.22 ± 0.21
1.35	585.9	527.1 ± 25.1	19.5	0.9290	4.97 ± 0.24 ± 0.21
1.375	617.2	538.9 ± 24.4	19.7	0.9324	4.75 ± 0.22 ± 0.20
1.4	610.3	461.6 ± 26.6	19.6	0.9356	4.12 ± 0.24 ± 0.18
1.425	585.2	437.0 ± 24.8	20.1	0.9305	3.99 ± 0.23 ± 0.17
1.45	464.6	338.5 ± 20.2	19.5	0.9248	4.04 ± 0.24 ± 0.17
1.475	612.6	483.2 ± 23.9	20.2	0.9177	4.25 ± 0.21 ± 0.18
1.5	746.4	584.0 ± 25.3	19.6	0.9093	4.39 ± 0.19 ± 0.19
1.525	491.5	395.2 ± 21.0	19.9	0.9033	4.47 ± 0.24 ± 0.19
1.55	575.0	465.1 ± 24.4	19.6	0.9013	4.58 ± 0.24 ± 0.20
1.575	524.3	441.2 ± 22.7	20.0	0.9026	4.66 ± 0.24 ± 0.20
1.6	455.6	464.2 ± 21.6	19.6	0.9072	5.73 ± 0.27 ± 0.25
1.625	528.1	472.5 ± 25.9	19.4	0.9167	5.03 ± 0.28 ± 0.22
1.65	492.5	403.2 ± 22.1	18.9	0.9350	4.64 ± 0.25 ± 0.20
1.675	469.6	297.9 ± 18.8	19.3	0.9508	3.45 ± 0.22 ± 0.15
1.7	482.2	237.6 ± 20.2	19.1	0.9735	2.65 ± 0.23 ± 0.11
1.725	519.4	208.5 ± 17.7	18.5	0.9928	2.18 ± 0.19 ± 0.09
1.75	522.9	176.0 ± 17.1	18.1	1.0080	1.85 ± 0.18 ± 0.08
1.775	486.9	150.9 ± 14.2	18.3	1.0150	1.66 ± 0.16 ± 0.07
1.8	418.8	81.3 ± 13.1	17.5	1.0170	1.08 ± 0.18 ± 0.05
1.825	516.1	119.6 ± 12.3	17.4	1.0120	1.31 ± 0.14 ± 0.06
1.85	431.2	95.4 ± 12.1	16.9	1.0030	1.30 ± 0.17 ± 0.06
1.87	655.8	103.3 ± 14.7	17.0	0.9901	0.93 ± 0.13 ± 0.04
1.89	616.0	71.1 ± 12.2	17.0	0.9893	0.68 ± 0.12 ± 0.03
1.9	493.9	83.3 ± 11.7	16.6	0.9837	1.03 ± 0.14 ± 0.04
1.925	619.5	63.3 ± 10.1	16.1	0.9721	0.65 ± 0.10 ± 0.03
1.95	425.3	31.7 ± 7.9	15.6	0.9614	0.49 ± 0.12 ± 0.02
1.975	502.8	51.7 ± 10.2	16.2	0.9477	0.66 ± 0.13 ± 0.03
2.0	577.1	72.1 ± 13.5	16.3	0.9405	0.81 ± 0.15 ± 0.03

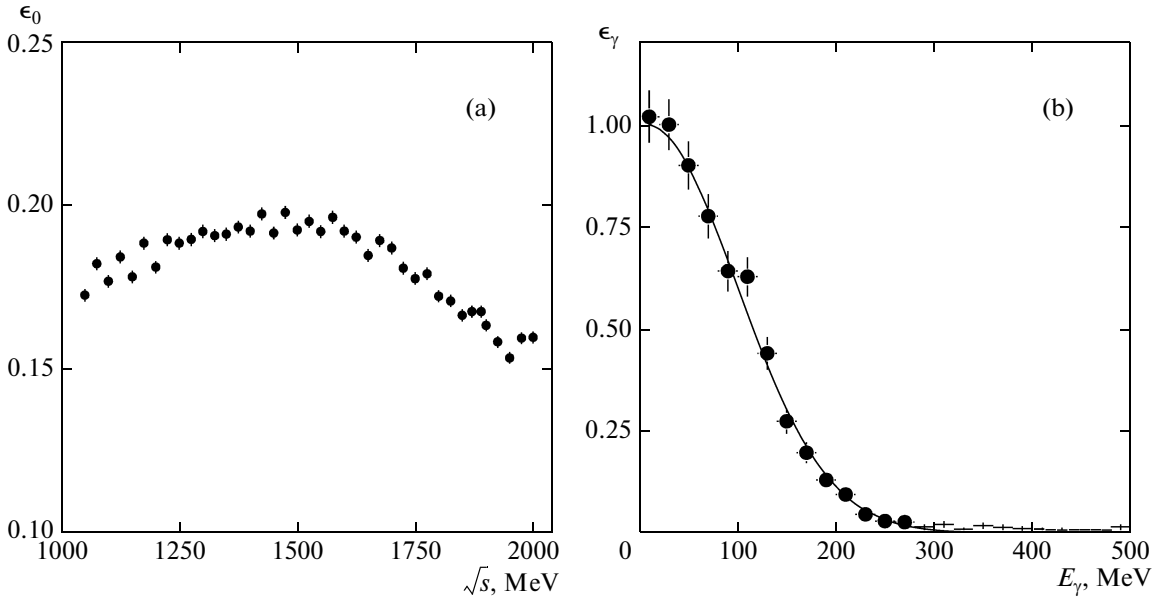

Fig. 2. (a) Simulated detection efficiency of the $e^+e^- \longrightarrow \pi^+\pi^-\pi^0$ process at $E_\gamma = 0$. (b) Dependence $\epsilon_\gamma(E_\gamma)$ for the energy $\sqrt{s}/2 = 700$ MeV approximated by a smooth line.

In order to obtain the experimental Born cross section, we used the following procedure. The experimental visible cross section is approximated by Eq. (4). In this case, the Born cross section is described by the sum of the contributions from vector resonances within the vector dominance model. The radiative corrections were calculated in the process of approximation of the model parameters. Then, the experimental Born cross section values were obtained using Eq. (5).

Under the assumption that the $e^+e^- \longrightarrow \pi^+\pi^-\pi^0$ process occurs through the intermediate $\rho\pi$ state, the Born cross section can be represented in the form

$$\sigma(s) = \frac{4\pi\alpha}{s^{3/2}}|A_{\rho\pi}|^2 P_{\rho\pi}(s), \qquad (6)$$

where $P_{\rho\pi}(s)$ is the function describing the energy dependence of the phase space factor of the $\rho\pi$ final state [10]. The amplitude $A_{\rho\pi}$ is represented as the sum of the contributions from four resonances and a nonresonance term:

$$A_{\rho\pi}(s) = \frac{1}{\sqrt{4\pi\alpha}}\left(\sum_{V=\omega,\phi,\omega',\omega''}\frac{\Gamma_V m_V^2\sqrt{m_V\sigma_V}}{D_V(s)\sqrt{P_{\rho\pi}(m_V^2)}} \times \exp(i\phi_V) + K\exp(i\phi_K)\right), \qquad (7)$$

where

$$D_V(s) = m_V^2 - s - i\sqrt{s}\Gamma_V(s), \qquad (8)$$

$$\sigma_V = \frac{12\pi B(V \longrightarrow e^+e^-)B(V \longrightarrow 3\pi)}{m_V^2}, \qquad (9)$$

m_V and $\Gamma_V(s)$ are the mass and energy-dependent total width of the V resonance, respectively; $B(V \longrightarrow e^+e^-)$ and $B(V \longrightarrow 3\pi)$ are the probabilities of the decays of this resonance into the e^+e^- and $\pi^+\pi^-\pi^0$ final states, respectively; and ϕ_V is the relative phase of interference between the V and $\omega(782)$ resonances. The energy dependence of the total width for the ω and ϕ resonances was calculated with the inclusion of all decay modes of these resonances whose contributions exceed 1%. It was assumed for the ω' and ω'' mesons that the energy dependence of the width is completely determined by their decays into the $\rho\pi$ final state. The parameters of the ω and ϕ mesons were taken from the tables [11]. The relative phase between the ω and ϕ mesons was assumed to be $\phi_\phi = 163°$ [10], and the phases of the ω' and ω'' excited states were fixed at 180° and 0°, respectively [12]. According to the results obtained with the BABAR detector [3], either an additional resonance or a nonresonance term should be added to the amplitude in order to describe the cross section above 1.8 GeV. In this work, the nonresonance complex amplitude $K\exp(i\phi_K)$ was added.

6. CORRECTIONS TO THE DETECTION EFFICIENCY

The systematic errors due to the inaccuracy of the simulation of the detector response to the events of the process under study were investigated using the exper-

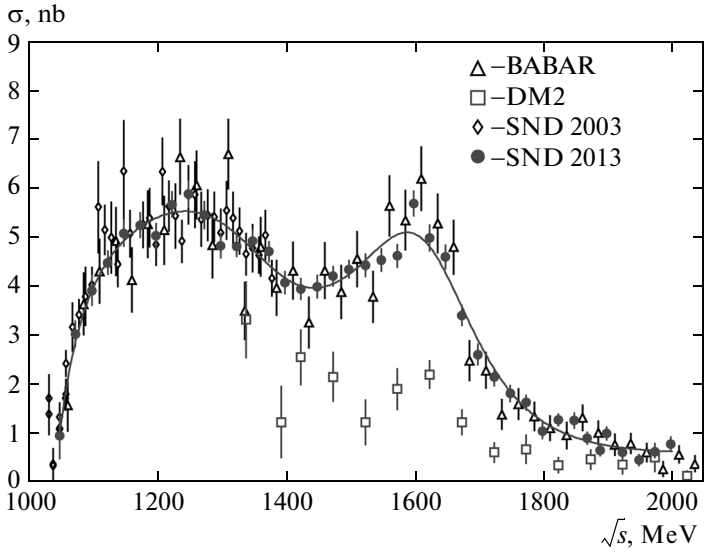

Fig. 3. Born cross section for the $e^+e^- \longrightarrow \pi^+\pi^-\pi^0$ process measured in this work (SND 2013) in comparison with the measurements in the experiments DM2 [1], SND at the VEPP-2M collider [2] (SND 2003), and BABAR [3]. The line is the approximation of the cross section by Eq. (7) with a nonzero nonresonance term.

imental data written in 2011 in the energy region of the ϕ-meson resonance. The cross section for the process under study is large in this energy range and the $e^+e^- \longrightarrow \pi^+\pi^-\pi^0$ events can be identified with weakened selection conditions and a low background level. The main background process $e^+e^- \longrightarrow K_SK_L$ with the decay $K_S \longrightarrow \pi^+\pi^-$ was suppressed by the condition imposed on the spatial angle between the charged particles $\psi < 140°$.

The correction to the detection efficiency was calculated from the ratio of the number of events in the data and simulation selected with the use of the standard ($N_{3\pi}$) and weakened ($N^*_{3\pi}$) constraints on the ith parameter:

$$\delta_i = \frac{(N_{3\pi}/N^*_{3\pi})_{\text{data}}}{(N_{3\pi}/N^*_{3\pi})_{\text{MC}}}. \qquad (10)$$

The conditions imposed on the number of photons in an event and on χ^2 of kinematic reconstruction appeared to be the most critical for this analysis. The correction $\delta_{\chi^2} = 0.958 \pm 0.005$ was obtained after the removal of the constraints imposed on χ^2. In order to obtain the correction to the condition $N_\gamma = 2$, we studied events with more than two photons. The kinematic reconstruction in these events was performed for all possible two-photon combinations. The combination with the minimal χ^2_E value was chosen. The resulting correction to the efficiency was

$$\delta_{N_\gamma} = 1.064 \pm 0.007 \pm 0.028,$$

where the first error is statistical and the second error is systematic, which includes the error in the simulation of the beam background (2%) and possible change of the correction value at the variation of the energy $\sqrt{s}$ from 1.02 to 2.00 GeV (2%). The second contribution was estimated as a change of the fraction of the events in the simulation that contain additional photons appearing because of the nuclear interaction of pions with the material of the detector. The resulting detection efficiency ϵ_0, which is the product of the efficiency obtained in the simulation ϵ_0^{MC} and the corrections δ_{χ^2} and δ_{N_γ}, is presented in Table 1. The total error of the detection efficiency including the above-described errors of the corrections and the statistical error of the simulation (1%) is 3.1%.

7. RESULTS AND DISCUSSION

The radiative corrections were calculated by Eq. (7). Table 1 summarizes the Born cross section and radiative correction values obtained in the approximation. The first and second errors in the measured cross section are statistical and systematic, respectively. The statistical error is determined by the error in the number of the selected events. The systematic error includes the uncertainty of the luminosity (2%), error in the detection efficiency (3.1%), error associated with the subtraction of the background (2%), and model uncertainty in the calculation of the radiative corrections. The last value was estimated when varying the parameters of the resonances and nonresonance term, within their errors. It does not exceed 1% at energies above 1.15 GeV. The total systematic uncertainty in this energy range is 4.3%. The radiative return to the ϕ-meson resonance makes a significant contri-

Table 2. Parameters of the ω' and ω'' resonances obtained in this work, in the experiment with the SND at the VEPP-2M collider (SND 2003) [10], and in the BABAR experiment [3]

	SND 2003	BABAR	This work
$m_{\omega'}$, MeV	$1400 \pm 50 \pm 130$	$1350 \pm 20 \pm 20$	1470 ± 50
$\Gamma_{\omega'}$, MeV	$870 \pm \begin{matrix}500\\300\end{matrix} \pm 450$	$450 \pm 70 \pm 70$	880 ± 170
$B(\omega' \longrightarrow e^+e^-)B(\omega' \longrightarrow \pi^+\pi^-\pi^0) \times 10^6$	$0.65 \pm 0.13 \pm 0.21$	$0.82 \pm 0.05 \pm 0.06$	0.73 ± 0.08
$m_{\omega''}$, MeV	$1770 \pm 50 \pm 60$	$1660 \pm 10 \pm 2$	1680 ± 10
$\Gamma_{\omega''}$, MeV	$490 \pm \begin{matrix}200\\150\end{matrix} \pm 130$	$230 \pm 30 \pm 20$	310 ± 30
$B(\omega'' \longrightarrow e^+e^-)B(\omega'' \longrightarrow \pi^+\pi^-\pi^0) \times 10^6$	$1.15 \pm \begin{matrix}0.44\\0.09\end{matrix} \pm 0.83$	$1.3 \pm 0.1 \pm 0.1$	1.56 ± 0.23

bution to the visible cross section at $\sqrt{s} \leq 1.15$ GeV. The radiative correction becomes large. Its model uncertainty also increases. Table 1 presents the range of the radiative correction for five points with $\sqrt{s} \leq 1.15$ GeV.

The resulting Born cross section is shown in Fig. 3 in comparison with the previous measurements and the approximation. It is seen that our data are the currently most accurate measurement of the cross section for the $e^+e^- \longrightarrow \pi^+\pi^-\pi^0$ process in the energy range of 1.05–2.00 GeV. They are in good agreement with the measurements with the SND at the VEPP-2M [2] and BABAR [3] and are inconsistent with the DM2-detector measurements [1].

In order to obtain the parameters of the excited resonances, the approximation was performed in a limited energy range below 1.8 GeV, where the cross section is well ($\chi^2/ndf = 37.5/32$) described by the sum of the contributions from four resonances ω, ϕ, ω', and ω'' without any nonresonance term. The parameters of the ω' and ω'' resonances obtained from the approximation of the cross section are presented in Table 2 in comparison with the previous experimental data.

The same model was used to describe the cross section in all three works. Since the ω' and ω'' resonances strongly overlap and interfere with each other and with the tails of the lower-lying ω and ϕ resonances, even a small change in the shape of the measured cross section can result in significant changes in the parameters of the approximation. This is seen from the comparison of our results with BABAR measurements [3]. A more accurate determination of the parameters of the resonances requires the simultaneous approximation of all data on the $e^+e^- \longrightarrow \pi^+\pi^-\pi^0$ cross section and the data on other isoscalar cross sections, e.g., $e^+e^- \longrightarrow \omega\pi^+\pi^-$.

8. CONCLUSIONS

The cross section for the $e^+e^- \longrightarrow \pi^+\pi^-\pi^0$ process in the energy range of 1.05–2.00 GeV has been measured in the experiment with the Spherical Neutral Detector at the VEPP-2000 collider. The data are in good agreement with previous measurements of this cross section in the experiments with the SND at the VEPP-2M [2] and BABAR [3], but have a better accuracy. The cross section for energies below 1.8 GeV is well described within the vector dominance model with the contributions from the ω, ϕ, ω', and ω'' resonances. Either an additional exited state or a nonresonance contribution should be added in order to describe the data above 1.8 GeV.

ACKNOWLEDGMENTS

This work was supported in part by the Ministry of Education and Science of the Russian Federation, by the Russian Foundation for Basic Research (project nos. 12-02-01250-a, 13-02-00418-a, 13-02-00375, 14-02-31375-mol-a, and 14-02-00129-a), and by the Council of the President of the Russian Federation for Support of Young Scientists and Leading Scientific Schools (project no. NSh-2479.2014.2).

REFERENCES

1. A. Antonelli, R. Baldini, M. E. Biagini, S. Calcaterra, and M. Schioppa, Z. Phys. C: Part. Fields **56**, 15 (1992).
2. M. N. Achasov, V. M. Aulchenko, K. I. Beloborodov, A. V. Berdyugin, A. G. Bogdanchikov, A. V. Bozhenok, A. D. Bukin, D. A. Bukin, S. V. Burdin, T. V. Dimova, V. P. Druzhinin, V. B. Golubev, V. N. Ivanchenko, A. A. Korol, S. V. Koshuba, et al., Phys. Rev. D: Part. Fields **66**, 032001 (2002).
3. B. Aubert, R. Barate, M. Bona, D. Boutigny, F. Couderc, Y. Karyotakis, J. P. Lees, V. Poireau, V. Tisserand, A. Zghiche, E. Grauges, A. Palano, M. Pappagallo, J. C. Chen, N. D. Qi, et al., Phys. Rev. D: Part., Fields, Gravitation, Cosmol. **70**, 072004 (2004).
4. Yu. M. Shatunov, A. V. Evstigneev, D. I. Ganyushin, et al., in *Proceedings of the Seventh European Particle Accelerator Conference, EPAC-2000, Vienna, Austria, June 26–30, 2000*, Ed. J. Poole and Ch. Petit-Jean-Genaz (European Physical Society, Geneva, 2000), p. 439.

5. M. N. Achasov, D. E. Berkaev, A. G. Bogdanchikov, D. A. Bukin, I. A. Koop, A. A. Korol, S. V. Koshuba, D. P. Kovrizhin, A. V. Otboev, E. A. Perevedentsev, Yu. A. Rogovsky, A. L. Romanov, P. Yu. Shatunov, Yu. M. Shatunov, D. B. Shwartz, et al., Nucl. Instrum. Methods Phys. Res., Sect. A **598**, 31 (2009); V. M. Aulchenko, A. G. Bogdanchikov, A. A. Botov, A. D. Bukin, D. A. Bukin, T. V. Dimova, V. P. Druzhinin, P. V. Filatov, V. B. Golubev, A. G. Kharlamov, A. A. Korol, S. V. Koshuba, A. E. Obrazovsky, E. V. Pakhtusova, V. M. Popov, et al., Nucl. Instrum. Methods Phys. Res., Sect. A **598**, 102 (2009); A. Yu. Barnyakov, M. Yu. Barnyakov, K. I. Beloborodov, V. S. Bobrovnikov, A. R. Buzykaev, A. F. Danilyuk, V. B. Golubev, V. L. Kirillov, S. A. Kononov, E. A. Kravchenko, A. P. Onuchin, K. A. Martin, S. I. Serednyakov, and V. M. Vesenev, Nucl. Instrum. Methods Phys. Res., Sect. A **598**, 163 (2009); V. M. Aulchenko, A. G. Bogdanchikov, A. A. Botov, D. A. Bukin, M. A. Bukin, E. A. Chekushkin, T. V. Dimova, V. P. Druzhinin, A. A. Korol, S. V. Koshuba, A. I. Tekutiev, and Yu. V. Usov, Nucl. Instrum. Methods Phys. Res., Sect. A **598**, 340 (2009).

6. S. Jadach, W. Placzek, and B. F. L. Ward, Phys. Lett. B **390**, 298 (1997).

7. S. Agostinelli, J. Allison, K. Amako, J. Apostolakis, H. Araujo, P. Arce, M. Asai, D. Axen, S. Banerjee, G. Barrand, F. Behner, L. Bellagamba, J. Boudreau, L. Broglia, A. Brunengo, et al., Nucl. Instrum. Methods Phys. Res., Sect. A **506**, 250 (2003).

8. S. Actis, A. Arbuzov, G. Balossini, et al. (Working Group on Radiative Corrections and Monte Carlo Generators for Low Energies Collaboration), Eur. Phys. J. C **66**, 585 (2010).

9. E. A. Kuraev and V. S. Fadin, Sov. J. Nucl. Phys. **41**, 466 (1985).

10. M. N. Achasov, K. I. Beloborodov, A. V. Berdyugin, A. G. Bogdanchikov, A. V. Bozhenok, A. D. Bukin, D. A. Bukin, T. V. Dimova, V. P. Druzhinin, V. B. Golubev, I. A. Koop, A. A. Korol, S. V. Koshuba, A. P. Lysenko, E. V. Pakhtusova, et al., Phys. Rev. D: Part. Fields **68**, 052006 (2003).

11. J. Beringer, J. F. Arguin, R. M. Barnett, et al. (Particle Data Group), Phys. Rev. D: Part., Fields, Gravitation, Cosmol. **86**, 010001 (2012).

12. A. B. Clegg and A. Donnachie, Z. Phys. C: Part. Fields **62**, 455 (1994).

Translated by R. Tyapaev